Using stable water isotopes to identify spatial-temporal controls on groundwater recharge in two contrasting East African aquifer systems.

Oiro Samson[1,*], Comte Jean-Christophe[1], Soulsby Chris[1] and Walraevens Kristine[2]

[1] University of Aberdeen, School of Geosciences, Scotland, United Kingdom.

[2]Ghent University, Department of Geology Laboratory for Applied Geology and Hydrogeology, Belgium.

Corresponding author: Samson.Oiro@abdn.ac.uk

Using stable water isotopes to identify spatial-temporal controls on groundwater recharge in two contrasting East African aquifer systems.

Abstract

Understanding the spatial-temporal variability in groundwater recharge is an essential prerequisite to sustainable management of aquifers. Spatial analysis of groundwater stable isotopes uncovered predominant controls on groundwater recharge in Nairobi Aquifer System (NAS) and South Coast aquifer (SC), two exemplar East-African aquifers relied upon by 7M people. 368 samples were analysed for stable isotopes and basic physico-chemical parameters. The NAS groundwater isotopes are controlled by precipitation orographic effects and enriched recharge from impounded lakes/wetlands. SC isotopes are correlated with water-table depth influencing evapotranspiration. Global Network of Isotopes in Precipitation-GNIP data revealed groundwater recharge during months of heavy rains in NAS, whilst SC experiences spatiotemporally diffuse recharge. Inferred 'isoscapes' show; in NAS, (1) direct, rapid recharge favoured by faults, well-drained soils and ample rainfall in uplands, (2) delayed recharge from impounded-lakes and wetlands in midlands, (3) focussed, event-based recharge in floodplains; in SC, diffuse recharge complicated by significant water-table evapotranspiration processes.

Key words:

Groundwater recharge, Stable isotopes, Aquifer systems, Meteoric water line, Evaporation effect

1: Introduction

Groundwater is an increasingly critical source of water for human use globally (Yoon *et al.* 2011, Liu *et al.* 2014, Kamtchueng *et al.* 2015, Zomlot *et al.* 2015). Groundwater resources provide a third of global fresh water supplies, accounting for 36% of domestic consumption, 42% of agricultural supplies and 27% of industrial use (Taylor *et al.* 2012). Aquifers supplying groundwater are increasingly becoming the main source of domestic water supply in Africa. Increasing water demand and projected climate change are expected to exacerbate over-reliance on groundwater for both domestic and agricultural supplies (Adelana et al., 2008; MacDonald et al., 2012; Taylor et al., 2012). Sub-Saharan Africa, including Eastern Africa, is endowed with substantial aquifers recharged by a tropical climate, but local communities suffer from scarcity of portable water supplies (Sambwa *et al.* 2009) and contamination, including salinization in coastal areas and islands (Comte *et al.* 2016). Groundwater is a critical resource component in Kenya, providing water supplies in many urban and rural areas, with Nairobi and the south Coast being the largest with over 7 million people depending on it as a supplementary source of water to piped water supply.

Groundwater recharge is facilitated by rainfall percolation through the unsaturated zone leading to replenishment of the saturated zone. Spatiotemporal variability in groundwater recharge is common due to the spatiotemporal variations in climatic conditions and land use as well as spatial heterogeneity of soil characteristics and aquifer properties (Raiber *et al.* 2015). Groundwater recharge quantitative decription is crucial to the assessment and sustainable use of groundwater resources (Lubis *et al.* 2008, Mair *et al.* 2013, Herrmann *et al.* 2015, von Freyberg *et al.* 2015). The importance of investigating groundwater recharge variability has grown over the last decade due to rising concerns over the impact of climate change and human activities on groundwater resources (Herrmann *et al.* 2015, Zomlot *et al.* 2015). A better

understanding of the timing and magnitude of groundwater recharge at the regional scale is crucial to more sustainable groundwater resource management (Scanlon *et al.* 2001, Cartwright and Morgenstern 2012). However, characterising spatial controls on groundwater recharge and hydrochemical evolution in inherently complex aquifers is challenging (Allocca *et al.* 2015, Raiber *et al.* 2015).

Application of stable isotope techniques for investigating water flow paths and storage dynamics has been an area of significant scientific advancement in recent decades (Lambs 2004, Carroll *et al.* 2008, Liu and Yamanaka 2012, Aggarwal *et al.* 2013, Kamtchueng *et al.* 2015). Groundwater isotope analysis is a useful tool for assessing the sources and rates of groundwater recharge, mapping out groundwater flow paths, reconstruction of past climates, quantifying of water fluxes across model boundaries and complementing climate models (Dansgaard 1964, Cerling *et al.* 1993, Gonfiantini *et al.* 2001, Bowen and Wilkinson 2002, Dettman *et al.* 2003, Kebede and Travi 2012, Mix *et al.* 2013). These advances have been driven by technological advances in laser spectroscopy that has rendered analysis for water stable isotope of oxygen and hydrogen both simple and inexpensive (Kamtchueng *et al.* 2015). These stable isotopes form natural tracers that are usually unaffected by geological interactions compared to the effect of phase changes (e.g. evaporation, condensation etc.) in hydrological systems (Liu *et al.* 2014). Following recharge, stable isotopes can approximate conservative tracers since the isotope values remain constant, so long as there is no fractionation or phase changes along the flow path making them suitable for identifying sources of groundwater recharge (Lambs 2004, Aggarwal *et al.* 2013, Liu *et al.* 2014). Characterising the stable oxygen and hydrogen isotope composition of groundwater can help develop an integrated understanding of how climatic, geographic, hydrological, geological and biological processes at both the surface and in the subsurface affect recharge sources, aquifer interconnectedness

and evapotranspiration influences (Lambs 2004, Carroll *et al.* 2008, Praamsma *et al.* 2009, Mix *et al.* 2013, Liu *et al.* 2014, Hemmings *et al.* 2015a, Raiber *et al.* 2015).

Using the concept of isoscapes can help answer questions concerning the origin/source of isotopic signatures observed in natural water analyses. Isoscapes are spatial patterns of isotopic compositions of precipitation over terrestrial areas are basically a function of fractionation of air masses moving inland over landscape (Kendall and Coplen 2001). Isoscapes can guide interpretation in defining controls influencing the eventual isotopic composition of groundwater from precipitation, recharge and groundwater movement in the subsurface (West *et al.* 2010)

For African aquifers, understanding of groundwater recharge is still highly fragmented (Kamtchueng *et al.* 2015), and most often limited to either continental or highly localised scales (Xu and Beekman 2003). This is explained by the sparse distribution and lack of synchronicity of groundwater recharge studies in Africa (e.g. MacDonald et al., 2012; and references therein) which limit comprehensive spatiotemporal analysis at the intermediate (local to regional) scale relevant to water resources management. East Africa is a region subject to adverse impacts of climate change and rapid groundwater development (Comte *et al.* 2016). In this study, stable isotopes are used to highlight the spatial variability of the recharge experienced in two contrasting Kenyan aquifer systems that are of great strategic importance for the wider region's development; the upland Nairobi volcanic-suite aquifer (NAS) and the South Coast (SC) sedimentary aquifer. The analysis focusses on identifying physical controls (environmental and anthropogenic) on groundwater recharge and flow processes. The main objectives are: (1) to identify and verify the source and origin of water recharging the groundwater of the two aquifer systems using water stable isotopes, (2) to provide insights on natural effects controlling water stable isotope compositions during and after recharge, (3) to explore the extent of human impacts on induced recharge from impounded lakes and wetlands in NAS area and seawater

intrusion through unsustainable groundwater abstraction and development along the coastal aquifers. The NAS is characteristic of volcanic aquifers encountered along the Great Rift Valley, spanning approximately 6000 km and over 10 countries across East Africa and the Arabic peninsula (from Lebanon in the farthest North to Mozambique in the farther South), on which 10s of millions of people are relying on for water supply. The SC aquifer is characteristic of sedimentary coastal aquifers occurring along the African eastern coast from Somalia to Mozambique (about 4000 km across four countries) that are also vital to both coastal communities and several major multimillion coastal cities (Mombasa, Dar Es Salaam, Maputo, Mogadishu). In addition, all these countries are affected by some of the highest population growth rates globally resulting in unprecedented, increasing water demand. The study therefore contributes to a better understanding of groundwater resources sustainability in Kenya, in the East African region and in ranges of volcanic and coastal sedimentary aquifer systems in the tropics.

2: Description of the study areas

Both study areas, the Nairobi Aquifer System (NAS) and the South Coast (SC) aquifer system, lie within the Athi catchment area of Kenya (Figure 1), one of the five Kenyan river basins. The Athi catchment borders the Tana Catchment Area (TCA) in the North, the Rift valley catchment area (RVCA) in the West, the Indian Ocean in the East, and Tanzania in the South. NAS altitude ranges between 1400 and 2600 masl (metres above sea level) while South Coast altitude ranges from 0 m to 500 masl.

2.1 Climatic Condition of the study sites

The NAS area experiences a subtropical highland climate. June/July season are the coldest months with some occasional periods with temperature dropping to 10 °C. The sunniest and warmest part of the year is from January to March, with an average temperature of 24 ºC. The mean average temperature for the year ranges between 22 °C to 25 °C. The NAS area experiences bimodal seasons of rainfall with higher precipitation occurring in March to May (May being the heaviest) and November with annual average precipitation of 1050 mm. The annual average percentage humidity ranges between 60% and 84% with higher percentages associated with seasons of heavy rains (see Fig. 2). Flooding problems are major issues during the wet season, particularly within residential areas and the lowland plains.

The SC aquifer area has an equatorial coastal climate with a mean maximum temperature of 30°C and a mean minimum of 23°C with annual average temperature ranging between 28°C and 31°C experiencing warm and humid conditions. October to April are the warmest months with an average maximum not exceeding 33ºC (Mwakamba et al., 2014). Humidity monthly average within the year ranges between 70% and 77%. The area experiences bi-modal rainfall distribution with the main wet season from April to June and the less pronounced short rains from October to December (see Fig. 2). The annual average precipitation at Waa station, within the study area amounts to 1100 mm with large variation in annual fluctuations. Surface water bodies (1986), linked inland gradual rainfall decrease to the prevalence of south-easterly winds illustrated by a pattern of isohyets parallel to the coast line.

2.2: Nairobi Aquifer System

The Nairobi volcanic-sedimentary aquifer system (NAS) is situated in deposits from two geological epochs, namely; the Tertiary epoch comprising of Kiambu trachyte, Nairobi phonolites, Athi tuffs & lake beds, Simbara basalts and Kapiti phonolites and the Pleistocene epoch constituted by deposits of Limuru trachyte, Tigoni trachyte, Karura trachyte, Kabete

168 trachyte, and Nairobi trachyte. The aquifer is overlying the poorly productive Pre-Cambrian
169 granitoid-gneiss basement system. Volcanic activity in the past controlled the geomorphologic
170 evolution of the area (Gaciri and Davies 1993). The NAS lithological succession includes
171 deposits of volcanic ashes and lavas (tuffs), whose thickness reaches approximately 400 m
172 beneath the city of Nairobi and gradually merges with the Tertiary deposits of the Athi
173 floodplain on the eastern side (Wamwangi and Musiega 2013). The Western boundary of the
174 NAS is structurally associated with the rift valley normal fracture systems having a general
175 North-South orientation along its flanks (Kuria 2013). Eastern and south-Eastern part are
176 occupied by the faultless floodplain of Athi sediments and Nairobi & Kapiti phonolites (altitude
177 of 1500 masl). The phonolites hydraulic properties are associated with primary open fissures
178 emanating from lava contraction during cooling processes. Saggerson (1991), estimated the
179 maximum thickness of the trachyte units (Nairobi trachyte, Kiambu trachyte, Mbagathi
180 phonolitic trachyte) to be 200 m though in some area (Tigoni and Limuru trachyte) ranges
181 between 75 m and 120 m of thickness (Limuru trachyte borehole geo-logs) (Odero 2011). Total
182 thickness of the volcanic units decreases towards the east where basement system outcrops.

183 The aquifer is characterised by a sequence of volcanic rocks, extensively faulted and displaced
184 against each other on the upper areas. Old land surfaces of different units, lake beds, solidified
185 contraction fissures and weathering along fractures amongst lava flows and ashes forms the
186 main aquifer system. Existing faults and structural discontinuities is likely promoting recharge
187 rates in the study area (WRMA, 2011). Complex regional faults/structures induce local
188 variations in aquifer hydraulic properties (Coleman *et al.* 2015, Dailey *et al.* 2015, Ochoa-
189 González *et al.* 2015). Faults can play two major contradicting roles with respect to
190 groundwater movement as it may promote or hinder preferential flows depending on whether
191 fractures are open and well-connected or closed/sealed, respectively (Bense and Person 2006,
192 Celico *et al.* 2006, Dewandel *et al.* 2006, Dailey *et al.* 2015). Geological formations of the

193 Upper Athi series form the main aquifer systems in the area with the transmissivity ranging
194 from 5 – 50 m^2/day (Okoth 2012). Faulted structures modify groundwater movement in the
195 area resulting in both lateral (NE and SW) and occasional longitudinal (N-S) flows (Odero
196 2011), see Fig. 3. (Kuria 2013) suggested that direct groundwater recharge from rainfall is
197 localised and favoured by faults zones and permeable volcanic soils. The infiltrated water
198 would percolate into deep-lying aquifers facilitated by faulting and fissure zones as
199 groundwater conduits (Okoth 2012, Kuria 2013).

200 ***2.3: South Coast aquifer system***

201 Geological mapping of the area was carried out by Gregory (1921), Miller (1952), Caswell
202 (1953), Thompson (1956) and Buckley (1981). Successive sedimentary deposits outcrop with
203 decreasing age (Jurassic to Pleistocene) in the direction of the Indian Ocean (Kuria 2013). The
204 general striking trends of sedimentary layers are parallel to the coastline on a SSW – NNE
205 direction and dipping to the east (Kuria 2013) (Fig. 4). Groundwater storage in the area is
206 geologically controlled. Two main exploited areas within the South Coast includes the Tiwi
207 and Msambweni aquifers. The Tiwi aquifer formation is the most productive and is composed
208 of Pliocene Magarini and Kilindini sands. These lithographic formations form part of the
209 Pleistocene reef complex encompassing the fossil reef and the back-reef lagoonal deposits
210 (Caruthers, 1985). The Pleistocene back-reef sand deposits (Kilindini Sands) exhibit the
211 uppermost groundwater potential in the Kenyan coast. The Kilindini facies comprises coarse
212 quartz sands, fine sands and coral limestone debris (Asurface water bodies, 1986). It shows
213 lateral variations due to textural changes and, in some cases, have been reworked (Coast Water
214 Service Board, 2009). It constitutes the so-called Tiwi aquifer (from the name of the village
215 where the main well field is sitting), a major water resource development area (Mwakamba *et*
216 *al.* 2014). The Kilindini and Kilindini-Magarini boundary sands exhibit favourable hydraulic
217 characteristics (with hydraulic conductivity, transmissivity and storativity all being high).

Mariakani sandstone, Mazeras sandstone and Maji ya Chumvi beds are associated with low boreholes yields only suitable for small-scale local supplies (Mwakamba *et al.* 2014).

3: Methodology

3.1: Groundwater sampling and in-situ water quality measurements

Spring water, wetland waters, rivers and groundwater were sampled for hydrogen (δD) and oxygen ($\delta^{18}O$) stable isotope analysis as shown on the maps above (Fig. 3 and Fig. 4). NAS samples were collected from all possible existing aquifer formations comprising of trachyte, phonolite, and lake bed sediments of Athi, while in SC most samples were collected from the most productive geological units of sands and karst limestone (Plio- to Pleistocene units) with few from older lower-yielding sandstones (pre-Pliocene units). The sampling procedure was similar to Sundaram et al. (2009); designing sampling plans, identifying logistical constraints and identifying the most suitable sampling points (boreholes, springs & surface water), recording sampling site conditions and taking water level measurements where possible. The sample bottles and equipment were thoroughly cleaned with distilled water prior to use and field equipment for measuring in-situ parameters was calibrated. On collection, sample bottles were labelled and where necessary filtered before transportation to the laboratory. Samples were collected in 500 ml plastic bottles and sub-samples in 7 ml vials were stored for isotope analysis. Vials were tightly filled and sealed with plastic caps before storage and refrigeration. In-situ measurement of basic water quality indicators as pH, EC (±0.1 µS/cm), TDS (±1 mg/l), Turbidity (±1 NTU), Salinity (±0.1 g/l), and Temperature (±0.1˚C) was conducted using portable kits from the Water Resources Management Authority and manufactured by WAGTECH. In total 254 and 116 samples were collected in NAS (February-March 2016) and SC (July 2016), respectively. Sample points were georeferenced using a hand-held GPS and

respective coordinates translated to GIS map and their elevation was derived using standard tools to extraction data from a DEM.

3.2: Stable Isotopes analyses

Samples collected for stable oxygen and hydrogen isotope analyses were stored in airtight 7 ml vials and refrigerated before being analysed at the University of Aberdeen using a Los Gatos DLT-100 laser isotope analyser (Los Gatos Research, Inc., San Jose, USA). The fourth generation Off-axis ICOS technology incorporated in this equipment yielded higher precision and reduced measurement time compared to conventional cavity ringdown spectroscopy (CRDS). The precision is set at ±0.1‰ and ±0.4‰ for oxygen ($\delta^{18}O$) and deuterium ($\delta^{2}H$) respectively, and all the isotopic ratio results reported as the δ-notation (‰) relative to the international VSMOW (Vienna Standard Mean Ocean Water) (Sharp et al., 2014).

3.3: GNIP data analysis and meteoric water line

Relevant Global Network of Isotope in Precipitation (GNIP) data was retrieved from International Atomic Energy Agency (IAEA) website in September 2016. GNIP data were collected between 1967 and 1968 for the two stations; 1) Muguga station in Nairobi (2030 masl), and 2) Dar es Salaam station (15 masl) in Tanzania as the nearest coastal station to Kenyan south coast. GNIP data was used in generating local meteoric water line (LMWL) providing the average relationship between hydrogen and oxygen stable isotopic composition of precipitation of a given coverage area (global, regional or local). The Global Meteoric Water Line (GMWL) was produced using the equation ($\delta D = 8.0\delta^{18}O + 10‰$) derived by Craig (1961) from precipitation data collected globally. Since Craig's model was designed for global datasets analysis, we use it in this work as a reference along with the trendline analysis of LMWLs, which are more fitting and site specific. By comparing the relationships between analysed stable isotope research samples and associating them with the derived relationships

provided for by GNIP LWML and GMWL equation, it provided insights in understanding processes affecting isotopic compositions during precipitation and recharge.

4: Results

4.1: Stable isotopic data relationship with meteoric water lines

Values of $\delta^{18}O$ and δD from NAS groundwater and spring samples range from -5.41 to -1.56‰ and -30.13 to -10.40‰ respectively. All samples (the majority being groundwater) from the South Coast for δ18O and δD are more enriched in heavier isotopes ranging from -3.63 to -0.08‰ and -16.62 to 1.53‰ respectively. The isotope ratios of $\delta^{2}H$ and $\delta^{18}O$ from the two aquifers are plotted in Figure 5 in relation to the GMWL and LMWL derived from the GNIP data from the Nairobi Station and Dar es Salaam station. Meteoric Water lines regression lines are expressed in (table 1) after Figure 5. The NAS isotopes reflect the upland recharge and generally show isotopically lighter water than the South Coast area (Dar es Salaam GNIP data). This disparity most likely reflects the rain out of heavier isotopes driven by air mass transformations through the altitude effect, distance from the coast, latitude and the precipitation amount (Dansgaard 1964) which results in depletion at high altitude. Coastal areas experience less rain out and its proximity to the evaporation source (Indian Ocean) ensures that the precipitation and recharge isotopes are characterised by enrichment with heavier isotopes compared to highland areas of NAS. To gain further insight into vapour isotope fractionation under different atmospheric conditions, the local meteoric water line (LMWL), and the Global Meteoric Water Line (GMWL) were considered (Figure 5).

Greater deviations from the meteoric lines are associated with higher evaporation experienced during moisture transfers in air masses and are linked to low humidity conditions which leads to kinetic fractionation. The higher the humidity the lower the evaporation rate. The deviation

289 of NAS data from both the GNIP LMWL and GMWL is greater compared with that of the SC.
290 This illustrates the multiple evaporation processes NAS moisture undergoes from precipitation
291 to eventual recharge compared to SC where moisture content in air masses is subjected to lesser
292 effects before precipitation and eventual recharge.

293 ***4.2: Sample type correlation with GNIP data***

294 Analyses of GNIP data (Figure 6a) reveals a dominance of recharge during the months of
295 March, April, May and November as precipitation isotopic signatures during these times are
296 similar to sampled borehole and spring waters in NAS. Other months show precipitation highly
297 enriched. Maybe due to the drier and warmer conditions, rainfall for these months does not
298 contribute significantly to groundwater recharge. Instead, most infiltrated water appears to be
299 lost through evapotranspiration (ET) as ET is greater than effective rainfall and its evaporation
300 is enhanced by low humidity and bare lands (no crop cover).

301 GNIP data from Dar es Salaam shows temporal variations over the year and it is not easy to
302 link specific months of precipitation driving recharge along the coast (Figure 6b). Stable
303 isotope values of rivers and other surface water bodies from both sites are more enriched than
304 those obtained from boreholes and springs. This suggests that there is no recharge of
305 groundwater by the rivers. Flowing river waters are subjected to evaporative fractionation
306 within the channels as it flows downstream making the water richer in heavy isotopes (Figure
307 6 c and d). Springs in both sites discharge groundwater from their respective areas, hence,
308 display similar isotope values.

309 ***4.3: Recharge characterization using isotopic composition***

310 Stable isotopes in sampled waters can be used as tracers to help identify different sources of
311 groundwater recharge (Butler 2007). Depleted isotope values plotting close to the MWL reflect
312 limited influence of evaporation thereby implying groundwater recharge origin from meteoric

waters (Rowley *et al.* 2001). Since the NAS groundwater is recharged by tropical rainfall, stable isotope results often plot above the global meteoric water line (i.e. depletion in ^{18}O) indicating the effects of moisture recycling as shown in Fig. 7. The effect of evaporation on recharge is evident in deviation from the global meteoric water line (GMWL) and points that plot below it.

Following the observed variation and irregular distribution of the isotopic composition of groundwater with respect to flow direction, δ^2H values points overlaying the river network suggested lack of direct infiltration of heavy isotope-enriched rivers into groundwater since the similarity between river water and sampled groundwater isotopes is not evident. This suggests that there is little or no direct infiltration from river channels into the groundwater system. However, groundwater in the central region of the NAS is enriched in deuterium providing evidence of evaporative fractionation in recharge waters. This region coincides with a high density of surface water bodies (impounded lakes and wetlands) (Figure 6) implying that these water bodies may induce groundwater recharge from impounded waters that are typically enriched in heavy isotope due to high evaporation of open waters. This delayed recharge of enriched surface water bodies water is consistent with the observed irregularity in isotopic distribution within the aquifer. There are over 120 impounded lakes and wetlands in the area with their surface area ranging from 400 m^2 to 400,000 m^2 with an average surface size of 45,000 m^2.

The eastern floodplains (Figure 7) are as depleted as the western mountain range suggesting preferential recharge of depleted rainfall. Depleted recharge results from the orographic effect (depleted rainfall) of the rift mountain range, however this effect is absent in the eastern low-land floodplains. Therefore, the groundwater signature observed is likely to be acquired through seasonal recharge during specific periods when rainfall is particularly depleted, i.e. the months of heavy rainfall (March, April, May, and November as shown in Figure 6a). As heavy

rainfall during these months is typically associated with floods in this area, we hypothesise that recharge takes place from rapid and focused infiltration of seasonal heavy rainfall and associated floods.

Overall, the spatial isotope maps within the NAS revealed three probable recharge scenarios; 1) preferential/direct recharge in the North and West facilitated by faults, permeable volcanic soil and high rainfall inputs with an altitudinally depleted isotope signature; 2) delayed induced recharge in the central part of the aquifer from impounded lakes and wetlands (with enriched isotope signatures); 3) focused groundwater recharge in the South and East associated with flooding in floodplains.

The SC aquifer isotope distribution is mostly controlled by a combination of direct and rapid infiltration from rainfall, seawater intrusion into active wells near the ocean, evaporation effects on shallow open wells (mainly towards the south), and high evapotranspiration effect due to shallow water-tables. The localized recharge is favoured by permeable sands and karstic coral limestones. Saline intrusion due to high abstraction and rising sea levels complicates conceptual understanding of groundwater movement at this site. Some wells under the influence of seawater intrusion and river samples experiencing backflows during high tides are enriched through water mixing with heavy isotope enriched ocean water. Open wells could be influenced by direct recharge during high intensity rainfall events, though the effect on our data is likely to be small as sampling was carried out during the dry season. However, shallow open wells are enriched with heavier isotopes compared to deeper hand-pumped wells and boreholes. This may be explained by both direct evaporation enriching the open wells and/or evaporation uptake from the vadose zone which then enriches recharge.

4.4: Isotopic composition relationship with depth to water table

Depth to water table relationship with stable isotopic composition values of groundwater samples is significant in zooming in at the effect of evapotranspiration in enriching groundwater with heavy isotopes. When water table and capillary fringe is near the surface, water table is subjected to evaporation. Evaporative fractionation effect is then experienced leading to the loss of lighter water stable isotopes of oxygen and hydrogen in the process, hence enriching groundwater with heavier component of stable isotopes. The stable isotope composition of NAS groundwater samples plotted against the depth to water table of respective sampling points yielded no relationship. Same procedure applied to SC samples produced a clear negative correlation (Fig. 8). In SC, the nearer the water table to the surface, the enriched groundwater stable isotopes of hydrogen and oxygen values are. The observation made in south coast is attributed to higher water table enabling effective evapotranspiration process to take place which modifies the composition of the stable isotopes.

4.5: Isotopic composition relationship with elevation/altitude

The elevation of recharge is usually evident from increasingly depleted isotope signatures in groundwater with increasing altitude, which in turn reflects altitudinal effects on precipitation (Hemmings *et al.* 2015b). This systematic variation is also affected by lower temperatures and higher relative humidity at altitude, wind and their lower influence on condensation and evaporation (Rowley *et al.* 2001). The stable isotope composition of groundwater in the NAS plotted against the elevation of the sampling well points reveals a relatively weaker linear correlation compared to correlation plot of both NAS and SC sample results plotted together, (Figure 9). A stronger correlation between $\delta^{2}H$ and elevation is evident compared to that of $\delta^{18}O$ with an isotopic lapse rate for NAS of 0.56‰/100 m and 0.15 ‰/100 m, respectively. SC isotopic lapse rates for $\delta^{2}H$ and $\delta^{18}O$ are 2.34‰/100 m and 0.35‰/100 m, respectively. However, when the samples of two sites are plotted together, a greater coefficient

385 determination of 45% for oxygen and 61% for hydrogen variation with elevation is achieved
386 compared to lower percentages of individual sites (see Fig. 9c compared to 9a and 9b). Isotopic
387 lapse rates for the combined data is 0.57‰/100 m and 0.08‰/100 m for both $\delta^{2}H$ and $\delta^{18}O$
388 respectively (Fig. 9c). Groundwater recharge at lower altitude is influenced by evaporation
389 effect compared to higher altitude due to lower percentage of humidity and higher temperature.
390 Evaporation causes fractionation in surface waters making them isotopically heavier. The
391 isotopic composition of orographic precipitation is probably constrained by the relationship
392 with elevation (Bershaw *et al.* 2016). The greater variability in 2H is more likely to simply
393 reflect its greater sensitivity to fractionation (e.g. evaporation) because of its small mass.

394 ***4.6: In-situ basic water quality parameters and distribution***

395 In the NAS, EC and TDS ranges are variable, ranging between 56 – 4380 µS/cm and 28 – 2192
396 ppm. The SC values have higher variability ranging between 86 -13920 µS/cm and 43 – 6960
397 ppm respectively, with the more concentrated samples indicating saline intrusion and increased
398 mineral dissolution along groundwater flow path due to rock-water interaction. The regional
399 distribution of EC at each site is shown in Figure 10. NAS EC values appear more lithologically
400 controlled through mineral dissolution (likely aluminosilicate and carbonate) favoured by high
401 groundwater residence times. Nairobi EC values increase along the line of the dominant
402 groundwater flow direction (West to East) i.e. reflecting increased groundwater residence
403 times, with the rift fault systems in the west likely acting as the main recharge zones sustained
404 by higher altitude and rainfall. The eastern region has lower elevation and slope gradients and
405 receives less rain compared to North-West. Areas where the Tertiary Athi sediment aquifer is
406 tapped, also produces higher EC compared to other volcanic formations due to presence of
407 highly soluble carbonate-rich mineral lake bed sediments. Electrical conductivity values in SC
408 increase towards the coastline, as anticipated, due to the seawater influence as well as carbonate
409 dissolution along the West to East dominant flow direction. However, they also increase

southwards towards the Tanzanian boarder which can be ascribed to higher temperatures (in the regional climatic gradient) driving higher evapotranspiration (Figure 10), as well as lithological influence as they are associated with the so-called 'Maji ya Chumvi sandstone' an older, less porous/permeable Permo-Triassic rock formations (Maji ya chumvi is a Swahili word for salty water). Maji ya Chumvi formation is characterised by low porosity/permeability as evidenced by very low borehole yield in this formation (Mwakamba *et al.* 2014). These properties favour thick capillary fringes resulting in high evapotranspiration thereby modifying the groundwater quality by increasing groundwater mineral concentration and enriching groundwater with heavy isotopes through the effect of evaporative fractionation. Increased mineral content contributes to higher EC values and salty nature of groundwater in this formation.

4.7: Isotopic composition relationship with electrical conductivity

The integration of isotope data and other water quality parameters like EC can help understand and upscale groundwater flow paths and recharge Observations made on Figure 11 however show no clear relationship, suggesting that processes influencing the isotopic composition of samples are effectively decoupled from rock-water interactions. This suggests that the existing isotopic composition is effectively preserving that of the recharge waters and subsequent effects of evaporative fractionation.

5: Discussion

Analysis and interpretation of the isotopic composition of these two important, but hydrogeologically and geographically contrasting aquifer systems provided a useful overview of the likely processes influencing groundwater recharge, patterns of groundwater movement and the likely influence of seawater intrusion and land use. However, as such, a broad overview excludes the more local influence of many internal and external controls on both groundwater

recharge and discharge which can only be fully understood through the integration of both physical and hydrogeochemical investigations, analysis and interpretation. For example, water quality reflects many potential mineral weathering sources which can only be characterised by full analysis of all major ions (Gastmans *et al.* 2016, Zhou *et al.* 2016); this is only crudely indexed by EC measurements and, apart from geothermal settings, has little direct link with stable water isotopes. Nevertheless, deep aquifer investigations using stable isotopes of hydrogen and oxygen provided useful insights into where recharge occurs since its composition is mostly affected by rainfall inputs and evaporative processes and not by hydrogeochemical reactions beneath the surface (Carroll *et al.* 2008, Hemmings *et al.* 2015b). Nevertheless, stable isotope investigations mainly provide information about recharge origin and not directly about the recharge rate (Liu *et al.* 2014), only a rough estimate for the latter.

Just as others (e.g. Gastmans et al., 2016; Mokadem et al., 2016; Zhou et al., 2016) have attributed groundwater chemistry to rock-water interactions and the imprint of human activities, this study also revealed that fractionation signatures of evaporation from man-made surface water bodies influence on the isotopic composition of groundwater within parts of the NAS. Such surface water bodies contribute to longer surface water residence times allowing evaporation effect to modify isotopic composition before infiltration. Increasing abstraction in the SC aquifer and tidal backflows into rivers has resulted in mixed fresh groundwater and seawater with marine isotopic signatures evident in the sampled wells in this area. This is consistent with the scenario reported by others (e.g. Petelet-giraud et al., 2016; Schmidt et al., 2011) in their study of monitored wells in Roussillon Basin, France. Such similarities can be used in advising water authorities operating along coastal lines anywhere in the world in planning their abstraction and monitoring networks. With the knowledge of direct and diffuse recharge along coastal areas aided by well-drained soils (sands), sand harvesting and waste

458 management (liquid and solid) along the coast can therefore be controlled to avoid negative
459 impact on groundwater system.

460 Groundwater recharge is a fundamental characteristic of regional hydrology (von Freyberg *et*
461 *al.* 2015). Its proper understanding is key to characterising and managing processes influencing
462 groundwater in any area, and particularly the renewable resource, which controls its
463 sustainability. The isotopic composition of these two contrasting aquifers in East Africa
464 provides an insightful initial framework for future work, such as the development of
465 quantitative modelling approaches. In particular, the delineated recharge zones inferred from
466 isotopes results can be used in assessing groundwater sensitivity to changes in recharge over
467 space and time or for quantitatively disentangling the relative importance of climate-induced
468 changes in recharge versus human-induced increase in abstraction. The study has provided a
469 simple, rapid and non-destructive method for understanding the key spatial controls on
470 groundwater recharge processes in the region. Where multi-disciplinary studies of groundwater
471 are involved, an initial evaluation with stable isotopes is an important first step in regional
472 studies. Findings from such reconnaissance can help in designing monitoring programmes and
473 identifying areas of specific interest concerning recharge. Monitoring networks and
474 groundwater management policies developed from this can be replicated in other areas within
475 the region. With such a clear distinction of recharge source signatures observed from the
476 analyses, focus and interest for more detail investigation can therefore be identified. Highlands
477 on both sides of the East African Great Rift Valley flanks, including the NAS, have almost
478 similar hydrogeological and hydrological environments, and are the source for many important
479 rivers emanating from groundwater-fed wetlands and springs. The coastal stripe stretching
480 from Somalia to Mozambique, through Kenya and Tanzania, also presents similar
481 hydrogeological characteristics (sedimentary rocks aquifers made of Pleistocene coral
482 limestone to Pliocene sands towards mainland) and undergo similar pressures and threats

(rapidly increasing groundwater demand due to high population growth rates and seawater intrusion issues) as the SC aquifer system. Observations made from comparing the NAS and SC aquifer systems provide useful insights for better conceptual understanding of other coastal and volcanic groundwater systems across East Africa as well as similar tropical regions beyond East Africa. At the African continental scale, coastal sedimentary and volcanic aquifers as studied here, along with large (intracontinental) sedimentary basins are the most relied upon groundwater resources.

6: Conclusion

NAS stable isotope results have shown the likely importance of induced groundwater recharge from surface water bodies except rivers, as well as direct recharge from seasonal rainfall in the uplands and in the lowlands flooding. The NAS stable isotopes composition appears to be more strongly influenced by the orographic effect of precipitation and evaporative fractionation effects on recharge from surface water bodies. In the SC aquifer, groundwater salinity increases towards the coastline, which is expected due to increasing seawater influence, but also southwards towards the Tanzanian border (increased evapotranspiration) promoted by the local climatic gradient and hydrogeological influence due to high evapotranspiration process experienced within maji ya Chumvi formation. Shallow open wells along the coast exhibit marked isotopic enrichment, an effect mainly influenced by enhanced evaporation in exposed hand-dug wells and the aquifer's shallow water table. NAS stable isotopic composition results shows three recharge scenarios: (i) along the western border, controlled by faults, well-drained volcanic soil and ample rainfall, (ii) the central area having high densities of impounding water bodies, where runoff is collected and retained aiding steady and continuous recharge of fractionated water, and (iii) induced and focused recharge promoted by flooding in flood plains along the eastern part. The latter is supported by Nairobi GNIP data and analysed isotopic

values that strongly suggest that recharge in the area mainly takes place during heavy rain months (March, April, May and November) when floods are common in the eastern low-lands. Due to well-drained sandy soils of the SC aquifer, recharge takes place throughout the year when it rains and not biased to specific periods. Protection of known localised groundwater recharge areas, groundwater recharge quantification, and managed aquifer recharge practices are needed for sustainable groundwater utilization and management. Fault lines/zones, impounded lakes and wetlands, and flood plains within NAS are targeted sites for protection as isotopic results reveal groundwater recharge emanates from them. The South Coast area is more complex as the soils over the entire area are well drained, and the water table is also high, thereby increasing pollution susceptibility. To protect contamination of recharging water, proper liquid waste management is key to preventing the leachates from finding their way into groundwater through recharge mechanisms. Over abstraction and poor development of wells where some are sunk into salty water have promoted saltwater intrusion. This can be reduced through the engagement of informed groundwater professionals in siting, designing and developing groundwater abstraction points.

Following the findings of this work, the following steps are recommended for future research; 1) geophysical investigation near man-made surface water bodies, springs, wetlands and across permanent rivers to investigate the extent and patterns of induced recharge and/or discharge, 2) physical coring and infiltration tests to establish the porosity and permeability of the top soil and saprolites to provide quantitative recharge estimates in the different zones of influence identified in Figure 6, 3) expanded major ions hydrogeochemical analyses and interpretation of groundwater samples for improving the understanding of groundwater quality and dominant processes to provide more insights on any rock-water interaction effect in NAS, 4) to carry out periodic sampling of rainwater, floodwater and surface water (rivers) over an entire hydrological year in an well-distributed network of observation sites for stable isotope analysis

to characterise aquifer – stream seasonal relationship, 5) Integrating all these processes and results in groundwater modelling for shaping a sustainable groundwater management plan.

Acknowledgements

We appreciate the financial support granted by the Royal Geography Society (with IBG), the Kenya Water Resources Management Authority (WRMA) and the University of Aberdeen. WRMA staff who assisted during groundwater sampling and J. Dick's assistance in running isotope laboratory tests are greatly acknowledged. We are grateful to two anonymous reviewers for their relevant comments and suggestions which have contributed to improve the manuscript.

References

Adams, B., 1986. Tiwi Aquifer Study, Final Report. *Prepared on behalf of British Geological Survey for the Ministry of Water Development, Kenya and British Technical Cooperation*.

Adelana, S.M., Macdonald, A.M., Adelana, S. and MacDonald, A., 2008. Groundwater research issues in Africa. *Applied Groundwater Studies in Africa, IAH Selected Papers on Hydrogeology*, *13*, pp.1-7.

Aggarwal, P.K., Cuntz, M., Davis, M.E., Edmunds, W.M., Froehlich, K.F.O., Gasse, F., Gat, J.R., Geyh, M.A., Gonfiantini, R., Gourcy, L.L., Groening, M., Hoffmann, G., Horita, J., Jouzel, J., Kaufman, A., Kerstel, E.R.T., Kharaka, Y.K., Lal, D., Loosli, H.H., Mariner, R.H., Mayer, B., McDonnell, J.J., Meijer, H.A.J., Michel, R.L., Moser, H., Plummer, L.N., Purtschert, R., Rauert, W., Rozanski, K., Thompson, L.G., Vitvar, T., and Werner, M., 2013. Isotopes in the Water Cycle Past, Present and Future of a Developing Science. Journal of Chemical Information and Modeling.

Allocca, V., De Vita, P., Manna, F. and Nimmo, J.R., 2015. Groundwater recharge assessment at local and episodic scale in a soil mantled perched karst aquifer in southern Italy. *Journal of Hydrology*, *529*, pp.843-853

.

Bense, V.F. and Person, M.A., 2006. Faults as conduit-barrier systems to fluid flow in siliciclastic sedimentary aquifers. *Water Resources Research*, *42*(5).

Bershaw, J., Saylor, J.E., Garzione, C.N., Leier, A. and Sundell, K.E., 2016. Stable isotope variations (δ 18 O and δD) in modern waters across the Andean Plateau. *Geochimica et Cosmochimica Acta*, *194*, pp.310-324.

Bowen, G.J. and Wilkinson, B., 2002. Spatial distribution of δ18O in meteoric precipitation. *Geology*, *30*(4), pp.315-318.

Butler II, T.W., 2007. Application of multiple geochemical indicators, including the stable isotopes of water, to differentiate water quality evolution in a region influenced by various agricultural practices and domestic wastewater treatment and disposal. *Science of the total environment*, *388*(1-3), pp.149-167.

Carroll, R.W., Pohll, G.M., Earman, S. and Hershey, R.L., 2008. A comparison of groundwater fluxes computed with MODFLOW and a mixing model using deuterium: Application to the eastern Nevada Test Site and vicinity. *Journal of hydrology*, *361*(3-4), pp.371-385.

582 Carruthers, R.M., 1985. Report on geophysical studies relating to the coastal aquifer of the
583 Mombasa District, Kenya.
584
585 Cartwright, I. and Morgenstern, U., 2012. Constraining groundwater recharge and the rate of
586 geochemical processes using tritium and major ion geochemistry: Ovens catchment,
587 southeast Australia. *Journal of hydrology*, *475*, pp.137-149.
588
589 Celico, F., Petrella, E. and Celico, P., 2006. Hydrogeological behaviour of some fault zones
590 in a carbonate aquifer of Southern Italy: an experimentally based model. *Terra Nova*, *18*(5),
591 pp.308-313.
592
593 Cerling, T.E., Wang, Y. and Quade, J., 1993. Expansion of C4 ecosystems as an indicator of
594 global ecological change in the late Miocene. *Nature*, *361*(6410), p.344.
595
596 Coleman, T.I., Parker, B.L., Maldaner, C.H. and Mondanos, M.J., 2015. Groundwater flow
597 characterization in a fractured bedrock aquifer using active DTS tests in sealed boreholes.
598 *Journal of Hydrology*, *528*, pp.449-462.
599
600 Comte, J.C., Cassidy, R., Obando, J., Robins, N., Ibrahim, K., Melchioly, S., Mjemah, I.,
601 Shauri, H., Bourhane, A., Mohamed, I. and Noe, C., 2016. Challenges in groundwater
602 resource management in coastal aquifers of East Africa: Investigations and lessons learnt in
603 the Comoros Islands, Kenya and Tanzania. *Journal of Hydrology: Regional Studies*, *5*,
604 pp.179-199.
605

606 Dailey, D., Sauck, W., Sultan, M., Milewski, A., Ahmed, M., Laton, W.R., Elkadiri, R.,
607 Foster, J., Schmidt, C. and Al Harbi, T., 2015. Geophysical, remote sensing, GIS, and
608 isotopic applications for a better understanding of the structural controls on groundwater flow
609 in the Mojave Desert, California. *Journal of Hydrology: Regional Studies*, *3*, pp.211-232.
610
611 Dansgaard, W., 1964. Stable isotopes in precipitation. *Tellus*, *16*(4), pp.436-468.
612
613 Dettman, D.L., Fang, X., Garzione, C.N. and Li, J., 2003. Uplift-driven climate change at 12
614 Ma: a long δ18O record from the NE margin of the Tibetan plateau. *Earth and Planetary*
615 *Science Letters*, *214*(1-2), pp.267-277.
616
617 Dewandel, B., Lachassagne, P., Wyns, R., Maréchal, J.C. and Krishnamurthy, N.S., 2006. A
618 generalized 3-D geological and hydrogeological conceptual model of granite aquifers
619 controlled by single or multiphase weathering. *Journal of hydrology*, *330*(1-2), pp.260-284.
620
621 Gaciri, S.J. and Davies, T.C., 1993. The occurrence and geochemistry of fluoride in some
622 natural waters of Kenya. *Journal of Hydrology*, *143*(3-4), pp.395-412.
623
624 Gastmans, D., Hutcheon, I., Menegário, A.A. and Chang, H.K., 2016. Geochemical evolution
625 of groundwater in a basaltic aquifer based on chemical and stable isotopic data: Case study
626 from the Northeastern portion of Serra Geral Aquifer, São Paulo state (Brazil). *Journal of*
627 *Hydrology*, *535*, pp.598-611.
628
629 Gonfiantini, R., Roche, M.A., Olivry, J.C., Fontes, J.C. and Zuppi, G.M., 2001. The altitude
630 effect on the isotopic composition of tropical rains. *Chemical Geology*, *181*(1-4), pp.147-167.

631

632 Hemmings, B., Gooddy, D., Whitaker, F., Darling, W.G., Jasim, A. and Gottsmann, J., 2015.
633 Groundwater recharge and flow on Montserrat, West Indies: Insights from groundwater
634 dating. *Journal of Hydrology: Regional Studies*, *4*, pp.611-622.

635

636 Herrmann, F., Keller, L., Kunkel, R., Vereecken, H. and Wendland, F., 2015. Determination
637 of spatially differentiated water balance components including groundwater recharge on the
638 Federal State level–A case study using the mGROWA model in North Rhine-Westphalia
639 (Germany). *Journal of Hydrology: Regional Studies*, *4*, pp.294-312.

640

641 Kamtchueng, B.T., Fantong, W.Y., Wirmvem, M.J., Tiodjio, R.E., Takounjou, A.F., Asai, K.,
642 Djomou, S.L.B., Kusakabe, M., Ohba, T., Tanyileke, G. and Hell, J.V., 2015. A multi-tracer
643 approach for assessing the origin, apparent age and recharge mechanism of shallow
644 groundwater in the Lake Nyos catchment, Northwest, Cameroon. *Journal of Hydrology*, *523*,
645 pp.790-803.

646

647 Kebede, S. and Travi, Y., 2012. Origin of the δ18O and δ2H composition of meteoric waters
648 in Ethiopia. *Quaternary international*, *257*, pp.4-12.

649

650 Kendall, C. and Coplen, T.B., 2001. Distribution of oxygen-18 and deuterium in river waters
651 across the United States. *Hydrological processes*, *15*(7), pp.1363-1393.

652

653 Kuria, Z., 2013. Groundwater distribution and aquifer characteristics in Kenya. In
654 *Developments in Earth Surface Processes* (Vol. 16, pp. 83-107). Elsevier.

655

Lambs, L., 2004. Interactions between groundwater and surface water at river banks and the confluence of rivers. *Journal of Hydrology*, *288*(3-4), pp.312-326.

Liu, Y. and Yamanaka, T., 2012. Tracing groundwater recharge sources in a mountain–plain transitional area using stable isotopes and hydrochemistry. *Journal of hydrology*, *464*, pp.116-126

.

Liu, Y., Yamanaka, T., Zhou, X., Tian, F. and Ma, W., 2014. Combined use of tracer approach and numerical simulation to estimate groundwater recharge in an alluvial aquifer system: A case study of Nasunogahara area, central Japan. *Journal of hydrology*, *519*, pp.833-847.

Lubis, R.F., Sakura, Y. and Delinom, R., 2008. Groundwater recharge and discharge processes in the Jakarta groundwater basin, Indonesia. *Hydrogeology Journal*, *16*(5), pp.927-938.

MacDonald, A.M., Bonsor, H.C., Dochartaigh, B.É.Ó. and Taylor, R.G., 2012. Quantitative maps of groundwater resources in Africa. *Environmental Research Letters*, *7*(2), p.024009.

Mair, A., Hagedorn, B., Tillery, S., El-Kadi, A.I., Westenbroek, S., Ha, K. and Koh, G.W., 2013. Temporal and spatial variability of groundwater recharge on Jeju Island, Korea. *Journal of hydrology*, *501*, pp.213-226.

679 Mix, H.T., Winnick, M.J., Mulch, A. and Chamberlain, C.P., 2013. Grassland expansion as
680 an instrument of hydrologic change in Neogene western North America. *Earth and Planetary*
681 *Science Letters*, *377*, pp.73-83.
682
683 Mokadem, N., Demdoum, A., Hamed, Y., Bouri, S., Hadji, R., Boyce, A., Laouar, R. and
684 Sâad, A., 2016. Hydrogeochemical and stable isotope data of groundwater of a multi-aquifer
685 system: Northern Gafsa basin–Central Tunisia. *Journal of African Earth Sciences*, *114*,
686 pp.174-191.
687
688 Mumma, A., Lane, M., Kairu, E., Tuinhof, A. and Hirji, R., 2011. Kenya groundwater
689 governance case study.
690
691 Mwakamba, C., Njuguna, A., Oiro, S., Ndung'u, A., Ang'weya, R., Hamisi, W., Mutinda, J.,
692 and Mwangi, S., 2014. *Tiwi Aquifer Water Resources Assessment Report*. Nairobi,
693 Kenya.
694 Ochoa-González, G.H., Carreón-Freyre, D., Cerca, M. and López-Martínez, M., 2015.
695 Assessment of groundwater flow in volcanic faulted areas. A study case in Queretaro,
696 Mexico. *Geofísica internacional*, *54*(3), pp.199-220.
697
698 Odero, D., 2011. *WATER RESOURCES MANAGEMENT AUTHORITY KENYA NATURAL*
699 *RESOURCES MANAGEMENT PROJECT STUDY OF GROUNDWATER RECHARGE*
700 *TO THE KIKUYU SPRINGS*. Nairobi, Kenya.
701 Owuor, S.O., Schüth, C., Lehné, R.J., Hoppe, A., Obiri, J., Nyaberi, D.M. and Kibet, M.K.,
702 2016. Estimation of hydraulic properties from pumping tests data of Nairobi area, Kenya.
703

Petelet-Giraud, E., Négrel, P., Aunay, B., Ladouche, B., Bailly-Comte, V., Guerrot, C., Flehoc, C., Pezard, P., Lofi, J. and Dörfliger, N., 2016. Coastal groundwater salinization: Focus on the vertical variability in a multi-layered aquifer through a multi-isotope fingerprinting (Roussillon Basin, France). *Science of the Total Environment*, *566*, pp.398-415.

Praamsma, T., Novakowski, K., Kyser, K. and Hall, K., 2009. Using stable isotopes and hydraulic head data to investigate groundwater recharge and discharge in a fractured rock aquifer. *Journal of Hydrology*, *366*(1-4), pp.35-45.

Raiber, M., Webb, J.A., Cendón, D.I., White, P.A. and Jacobsen, G.E., 2015. Environmental isotopes meet 3D geological modelling: conceptualising recharge and structurally-controlled aquifer connectivity in the basalt plains of south-western Victoria, Australia. *Journal of Hydrology*, *527*, pp.262-280.

Rowley, D.B., Pierrehumbert, R.T. and Currie, B.S., 2001. A new approach to stable isotope-based paleoaltimetry: implications for paleoaltimetry and paleohypsometry of the High Himalaya since the Late Miocene. *Earth and Planetary Science Letters*, *188*(1-2), pp.253-268.

Sambwa, A., Nnamdi, N.D. and Ebelechukwu, U.S., 2009. Recycling of used DC motors as solar pumps for water supply and water delivery applications in urban poor and rural communities in sub-Saharan Africa. *Desalination*, *248*(1-3), pp.586-594.

728 Scanlon, B.R., Healy, R.W. and Cook, P.G., 2002. Choosing appropriate techniques for
729 quantifying groundwater recharge. *Hydrogeology journal*, *10*(1), pp.18-39.
730
731 Schmidt, A., Santos, I.R., Burnett, W.C., Niencheski, F. and Knöller, K., 2011. Groundwater
732 sources in a permeable coastal barrier: Evidence from stable isotopes. *Journal of hydrology*,
733 *406*(1-2), pp.66-72.
734
735 Sundaram, B., Feitz, A., de Caritat, P., Plazinska, A., Brodie, R.S., Coram, J. and Ransley, T.,
736 2009. Groundwater sampling and analysis–a field guide. *Geoscience Australia, Record*,
737 *27*(95).
738
739 Taylor, R.G., Scanlon, B., Döll, P., Rodell, M., Van Beek, R., Wada, Y., Longuevergne, L.,
740 Leblanc, M., Famiglietti, J.S., Edmunds, M. and Konikow, L., 2013. Ground water and
741 climate change. *Nature Climate Change*, *3*(4), p.322.
742
743 Tole, M.P., 1997. Pollution of groundwater in the coastal Kwale District, Kenya. *IAHS*
744 *Publications-Series of Proceedings and Reports-Intern Assoc Hydrological Sciences*, *240*,
745 pp.287-310.
746
747 von Freyberg, J., Moeck, C. and Schirmer, M., 2015. Estimation of groundwater recharge and
748 drought severity with varying model complexity. *Journal of Hydrology*, *527*, pp.844-857.
749
750 Vouillamoz, J.M., Lawson, F.M.A., Yalo, N. and Descloitres, M., 2015. Groundwater in hard
751 rocks of Benin: Regional storage and buffer capacity in the face of change. *Journal of*
752 *Hydrology*, *520*, pp.379-386.

Wamwangi, E. and Musiega, D., 2013. Geospatial Analysis of Groundwater Fluoride Contamination in Embakasi Area, Nairobi GEOSPATIAL ANALYSIS OF GROUNDWATER FLUORIDE CONTAMINATION IN EMBAKASI AREA , NAIROBI, 1–15.

West, J.B., Bowen, G.J., Dawson, T.E. and Tu, K.P. eds., 2009. *Isoscapes: understanding movement, pattern, and process on Earth through isotope mapping*. Springer Science & Business Media.

Xu, Y. and Beekman, H.E. eds., 2003. Groundwater recharge estimation in Southern Africa.

Yoon, H., Jun, S.C., Hyun, Y., Bae, G.O. and Lee, K.K., 2011. A comparative study of artificial neural networks and support vector machines for predicting groundwater levels in a coastal aquifer. *Journal of Hydrology*, *396*(1-2), pp.128-138.

Zhou, J., Zhang, Y., Zhou, A., Liu, C., Cai, H. and Liu, Y., 2016. Application of hydrochemistry and stable isotopes (δ34S, δ18O and δ37Cl) to trace natural and anthropogenic influences on the quality of groundwater in the piedmont region, Shijiazhuang, China. *Applied Geochemistry*, *71*, pp.63-72.

Zomlot, Z., Verbeiren, B., Huysmans, M. and Batelaan, O., 2015. Spatial distribution of groundwater recharge and base flow: Assessment of controlling factors. *Journal of Hydrology: Regional Studies*, *4*, pp.349-368.

Table 1: Meteoric Water Lines (MWL) equation table generated from the regression analysis/lines producing different values of D-excesses, line slopes (a)/$\delta^{18}O$ coefficients with respect to each data sets, and their respective r^2 values.

Data Source	**δD**	**Line slopes (a)**	**D-excesses (b)**	**MWL Equation $\delta D = a*\delta^{18}O + b$**	**r^2**
GMWL	1	8	10	$\delta D = 8.0*\delta^{18}O + 10‰$	1
Dar es Salam GNIP δ (‰)	1	7.04365	6.8837451	$\delta D = 7.04*\delta^{18}O + 6.9‰$	0.84993
Nairobi GNIP δ (‰)	1	8.03614	14.641321	$\delta D = 8.04*\delta^{18}O + 14.6‰$	0.93816
NAS groundwater δ (‰)	1	1.82746	-13.073984	$\delta D = 1.83*\delta^{18}O - 13.1‰$	0.14628
SC groundwater δ (‰)	1	5.34425	3.6973505	$\delta D = 5.34*\delta^{18}O + 3.7‰$	0.87803

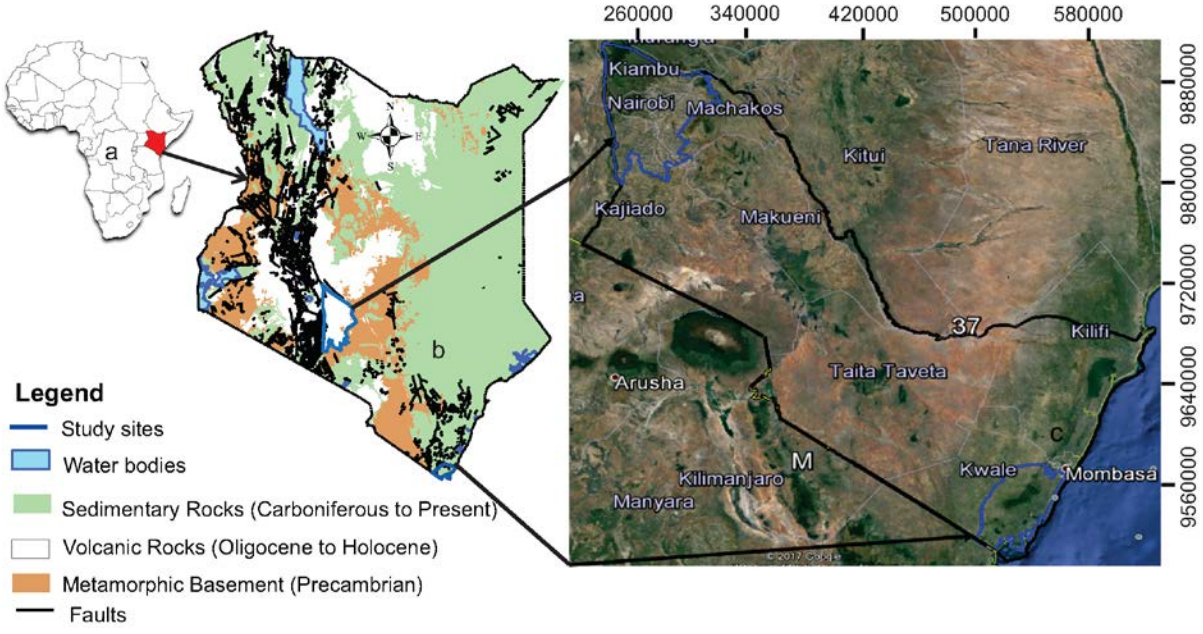

Figure 1: (a) Map of Africa showing location of Kenya in red, (b) Simplified Geological map of Kenya showing distribution of the three main bedrock types: Volcanic, Sedimentary and Metamorphic, and (c) Location map of the two strategic aquifers under study (blue outline) within the Athi Catchment Area (black outline) with major County administrative boundaries.

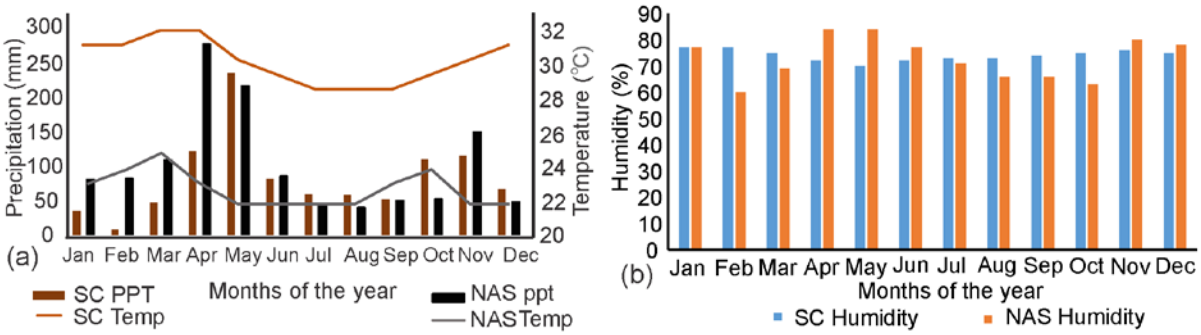

Figure 2: (a) Column charts illustrating the variation averages of precipitation (ppt in mm) and line charts demonstrating the monthly average temperatures over the year on both sites, and (b) Column charts showing humidity (%) variations over the months in the year for both Nairobi aquifer system area (NAS) and South Coast aquifer system (SC).

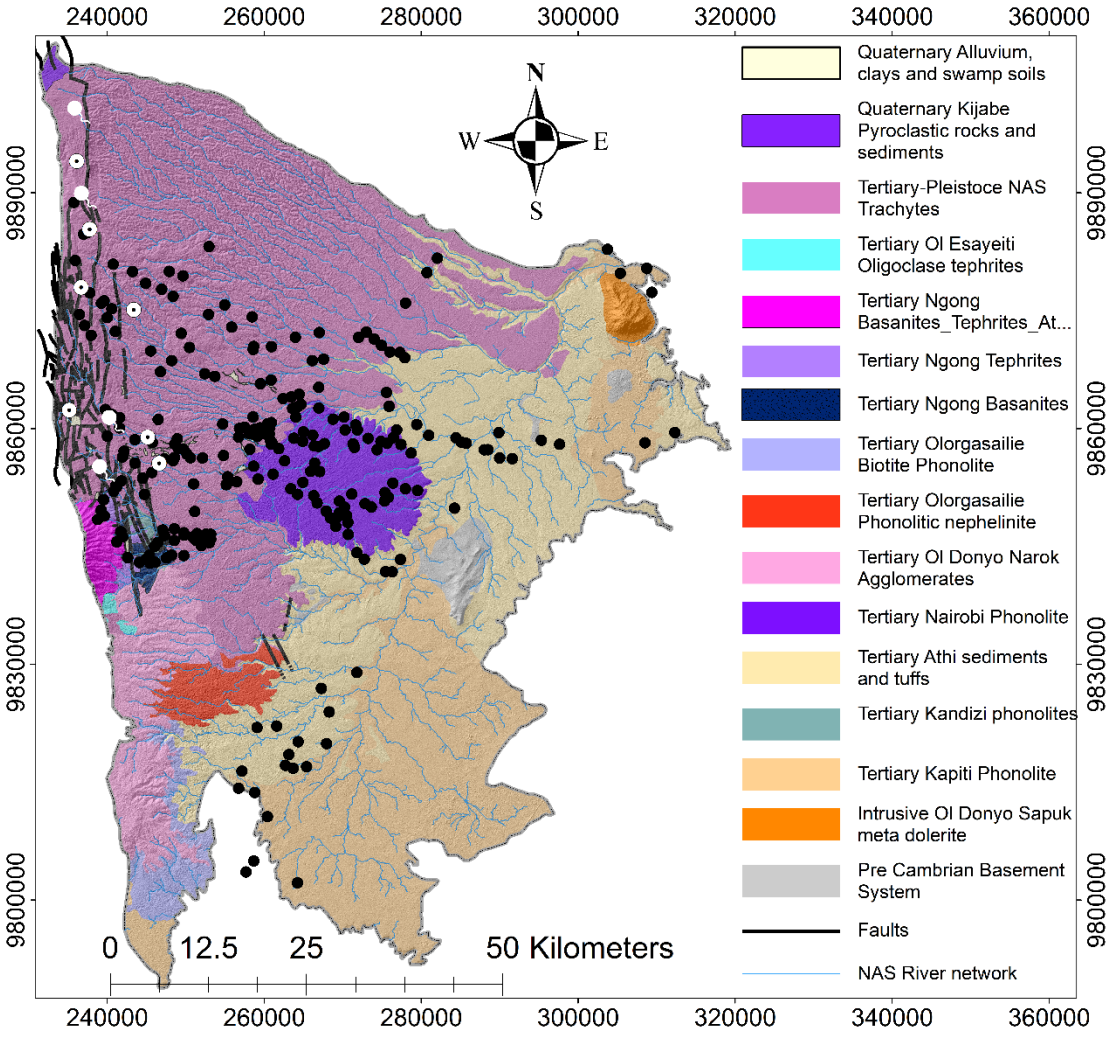

Figure 3: Simplified Nairobi aquifer System geological map with river networks and isotope water sampling points (boreholes in black, springs in white filled markers, and surface water (wetlands, rivers and surface water bodies) in dotted white.

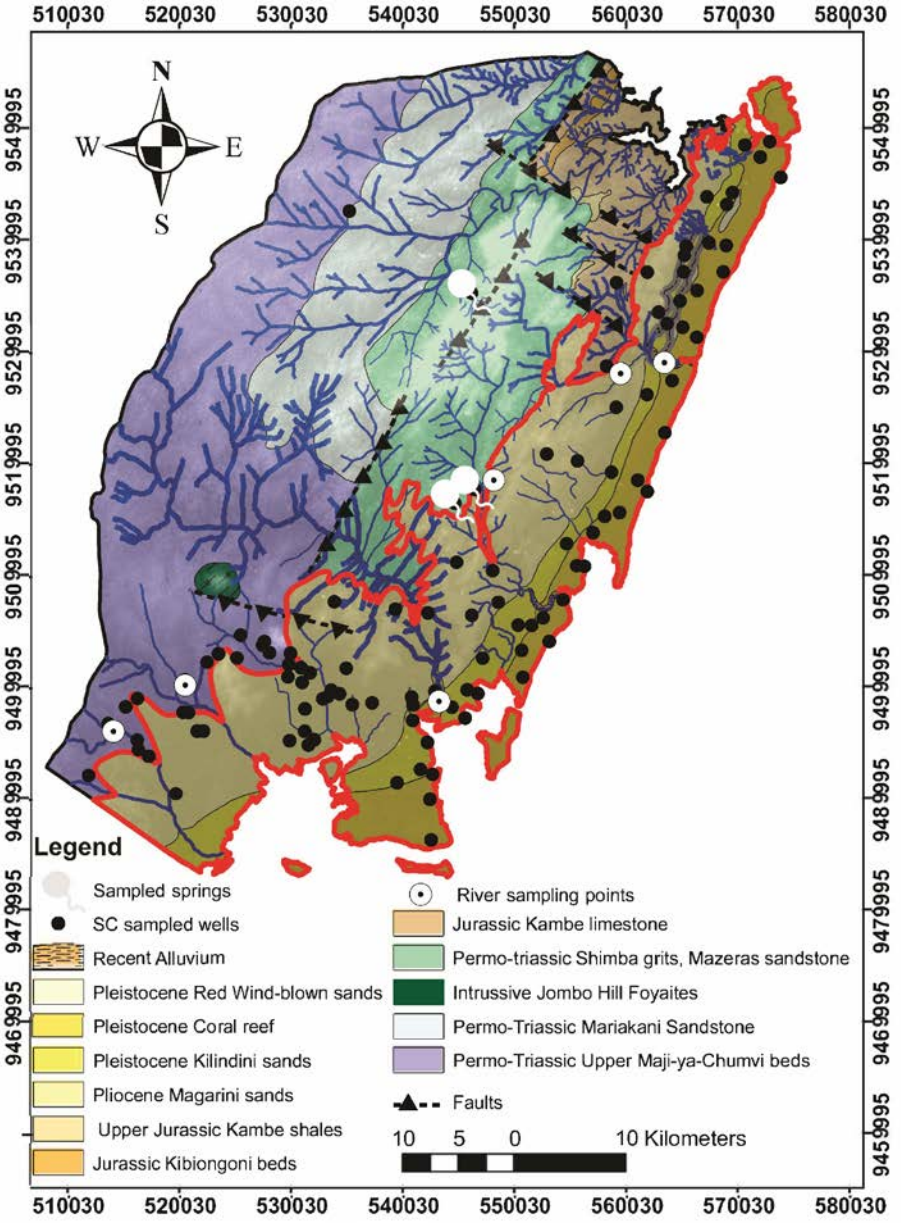

Figure 4: South Coast Study Area geological map with isotope water sampling sites (boreholes and wells in black points, springs in in white tailed markers, and rivers in dotted white) overlying DEM hill shade of the area with main productive aquifer coverage area demarcated in red.

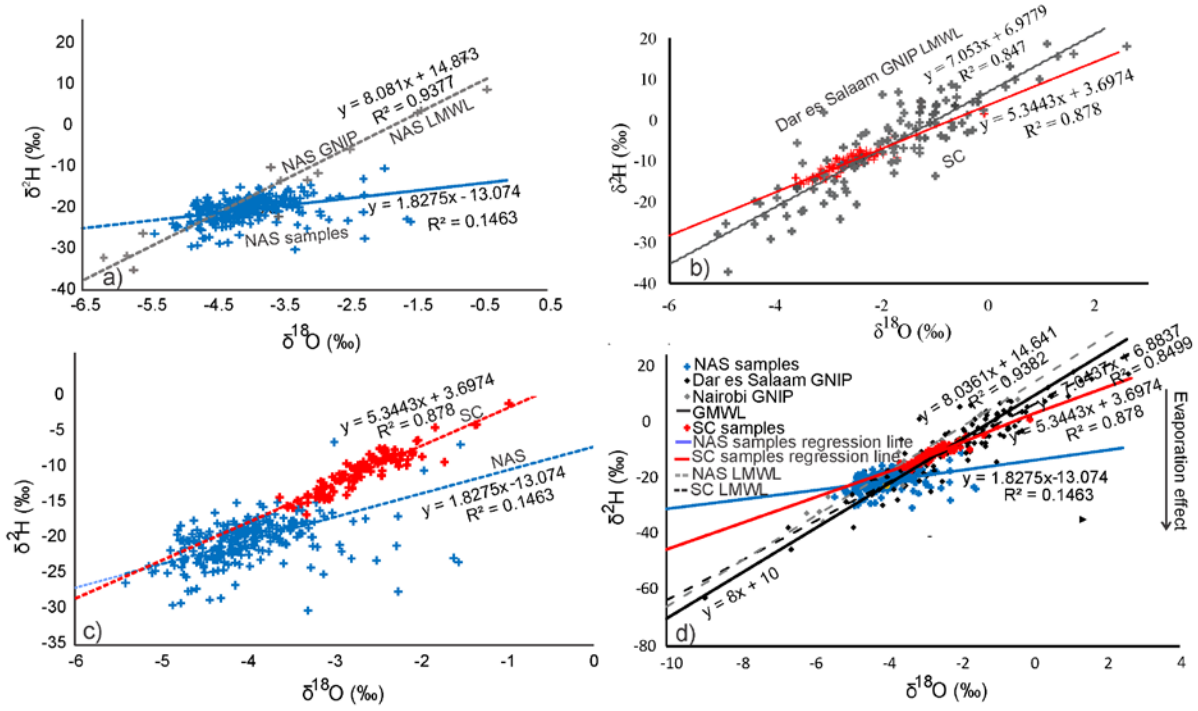

Figure 5: (a) a plot of NAS isotopic values in relation with locally derived meteoric water line using local GNIP data from Muguga station in Nairobi, indicating that samples collected had experienced severe evaporative fraction effect, (b) SC isotopic values in relation to the closest GNIP station data from Dar es Salaam showing that SC samples reflect water source might have gone through moisture recycling before precipitation and recharging the aquifer, (c) a plot of NAS and SC sample showing SC samples enriched with heavy isotope compared to NAS samples, and (d) a plot of all the categories of analyzed, derived and retrieved data of isotopic composition with their respective regression lines. SC samples are enriched compared to NAS (isotopic composition values data), GNIP data are well spread and showing a clear influence of tropical rains as Nairobi GNIP plots almost on the right side of the GMWL and are almost in line with GMWL (units in ‰).

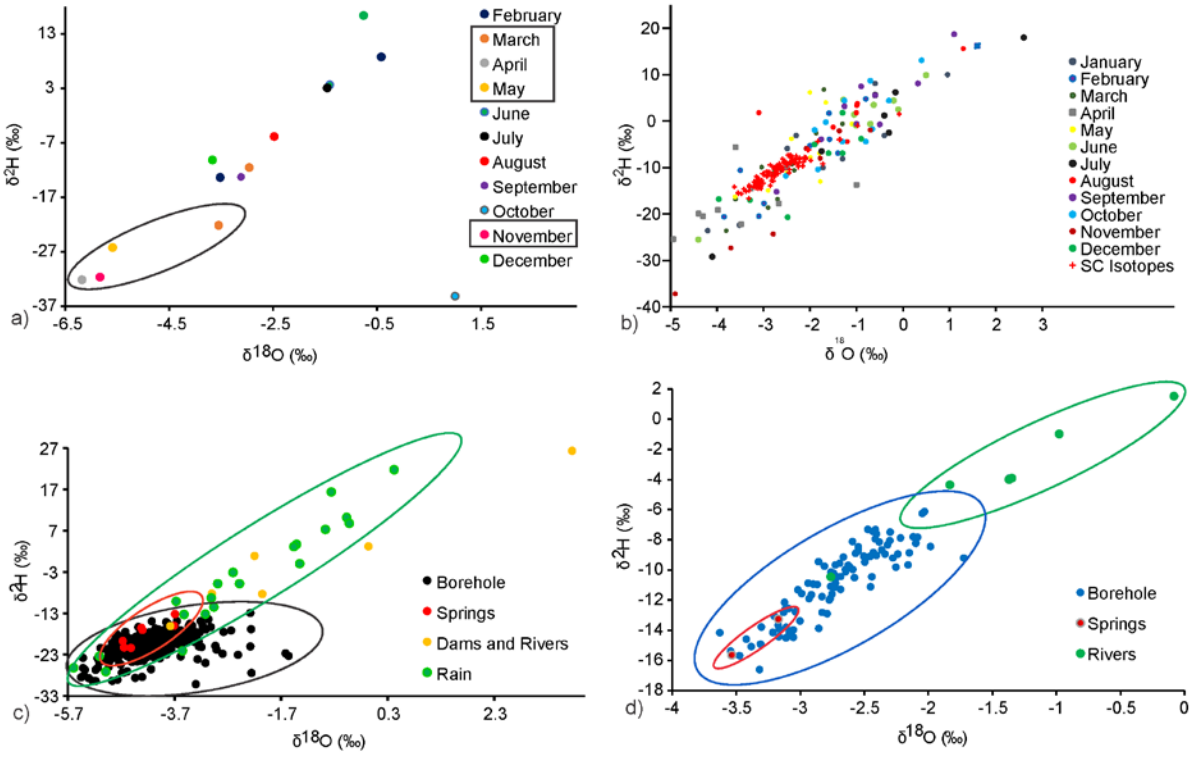

Figure 6: (a) GNIP stable isotope composition for respective months of precipitation depicting (in black ellipse) months of precipitation whose signatures are observed in NAS sampled groundwater, reflecting direct recharge, (b) SC isotopic values plotted together with Dar es Salaam GNIP data for understanding recharge months, (c) Comparison of categorized NAS isotopic composition to show strong link between springs and borehole samples while surface water bodies are associated with heavy isotopes and rains during dry seasons associated with heavier isotopes, and (d) SC categorized samples revealing association between springs and wells which contrasts with river waters possessing enriched isotopes due to tidal backflows.

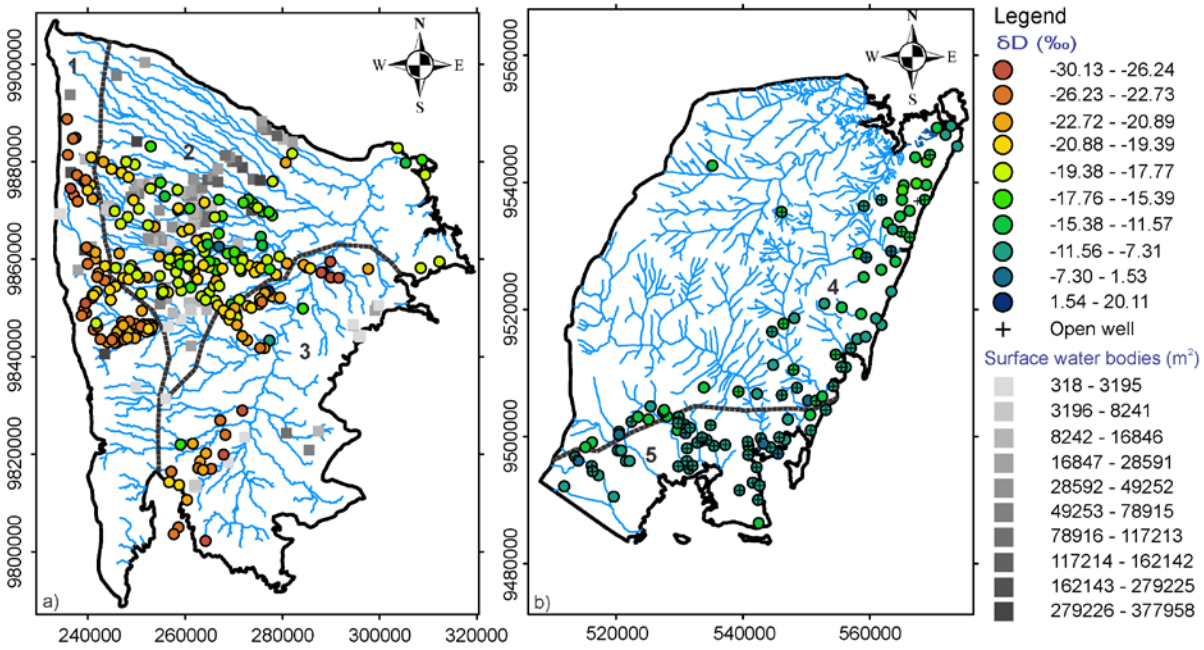

Figure 7: (a) Isotopic composition distribution within NAS delineating different possible recharge zones correlating with the river network and surface water bodies; (1) preferential recharged favoured by faults and good volcanic soil (heavy isotope depletion), (2) deferred/delayed induced recharge due to surface water bodies retention (enrichment) in impounded lakes and wetlands, and (3) focused seasonal recharge promoted by perennial flooding during heavy rains (depletion); (b) SC stable isotopic composition distribution within the area demonstrating (4) opposite influence of seawater intrusion (heavy isotope enrichment) and direct recharge from precipitation (depletion), and (5) additional effect of climatic gradient (increased temperature and evapotranspiration) and the open well effect (direct evaporation and evaporative uptake from the vadose zone and shallow water table).

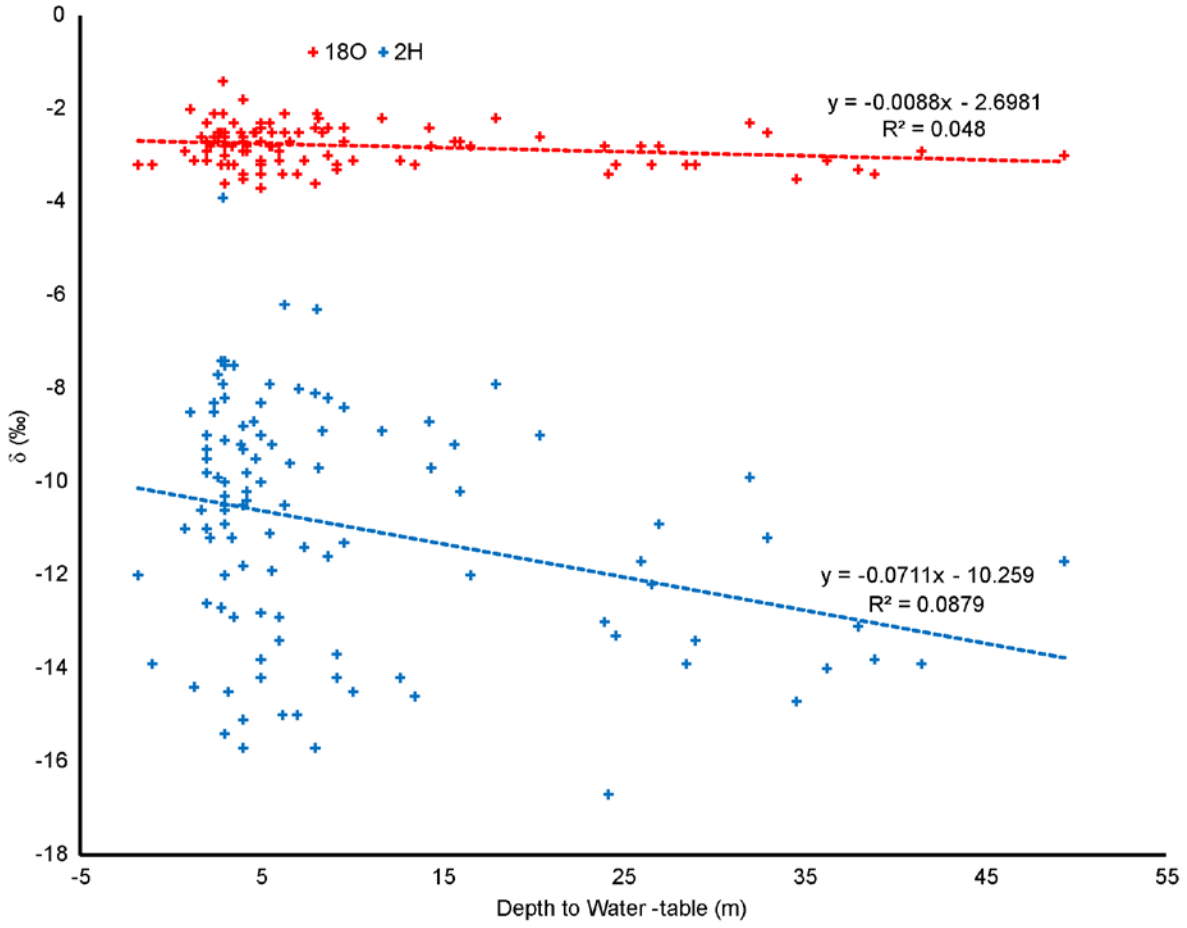

Figure 8: Correlation between δ18O and δ2H of South coast samples (units in ‰) with respect to water table depth of their respective sampling wells.

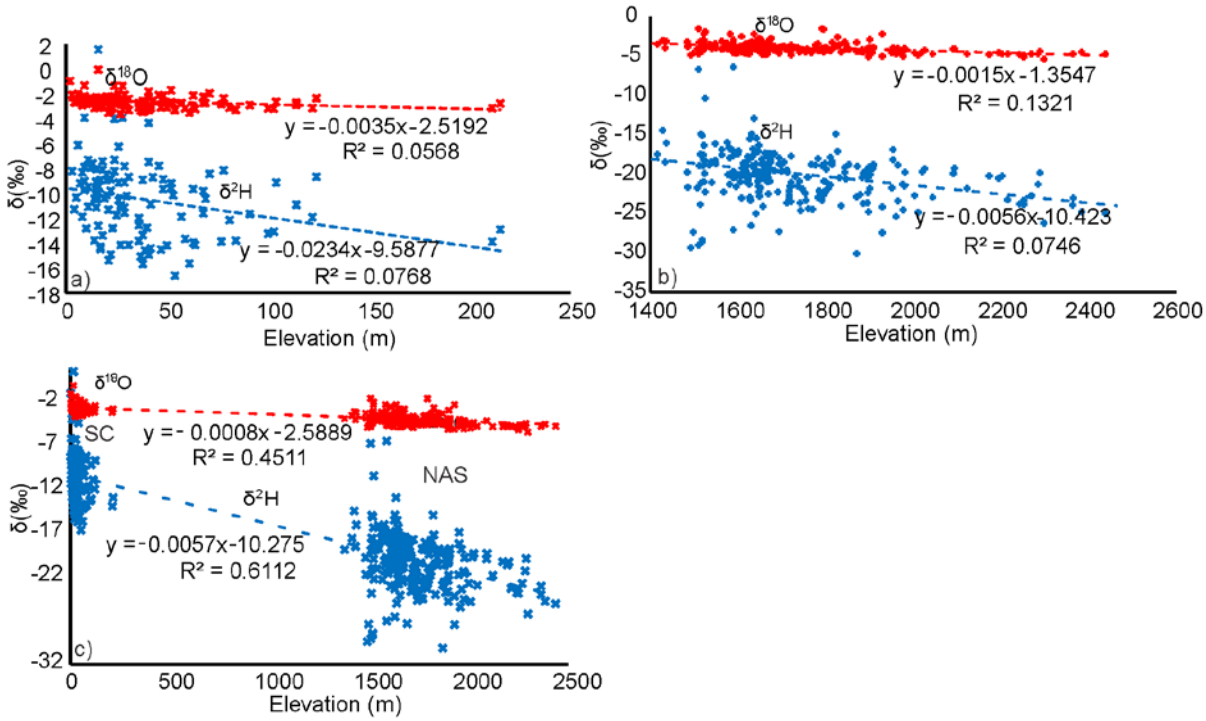

Figure 9: Correlation between δ18O and δ2H of, (a) South coast samples (units in ‰) with their sampling elevation points, (b) NAS samples (units in ‰) with their water sampling point elevations, and (c) Combined samples for both sites plotted against their sampling elevation points (elevation measured above mean sea level).

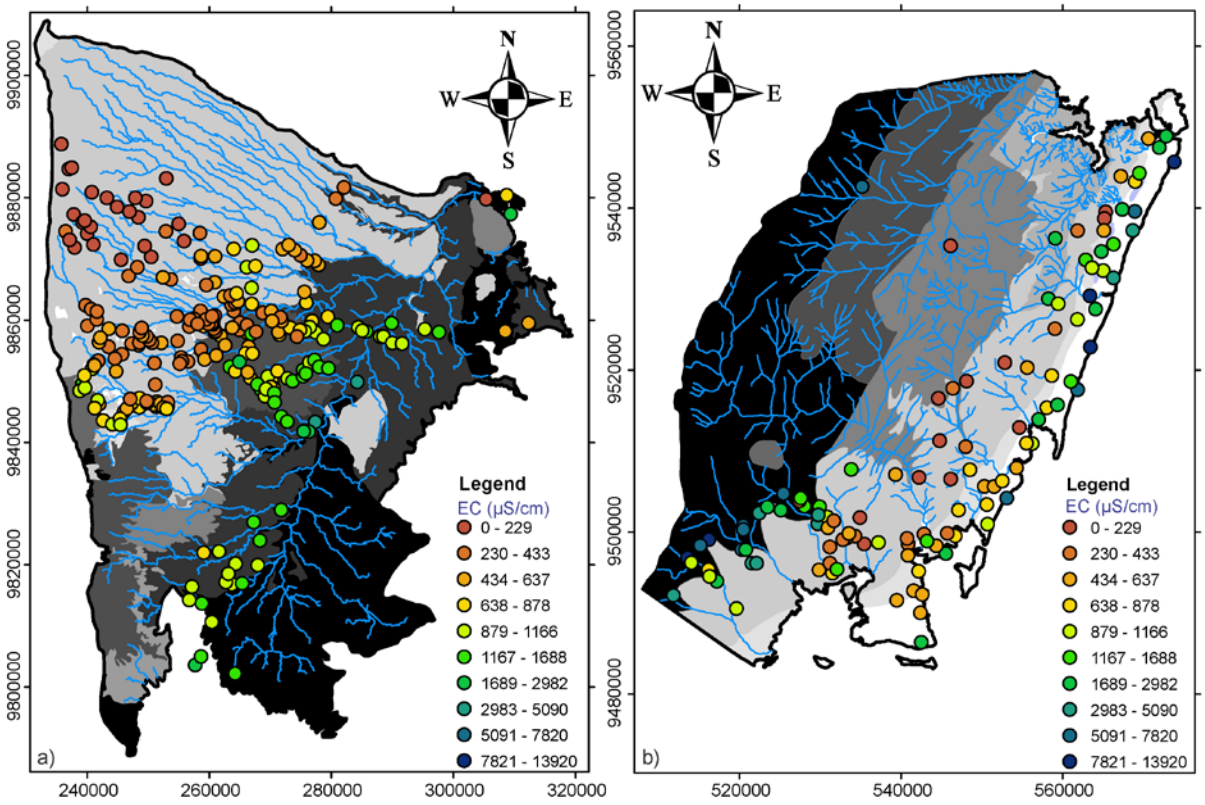

Figure 10: Spatial distribution of Electrical Conductivity (µS/cm) observations for the two study areas measured with background geology (see geology legend on Figure 2 and 3).

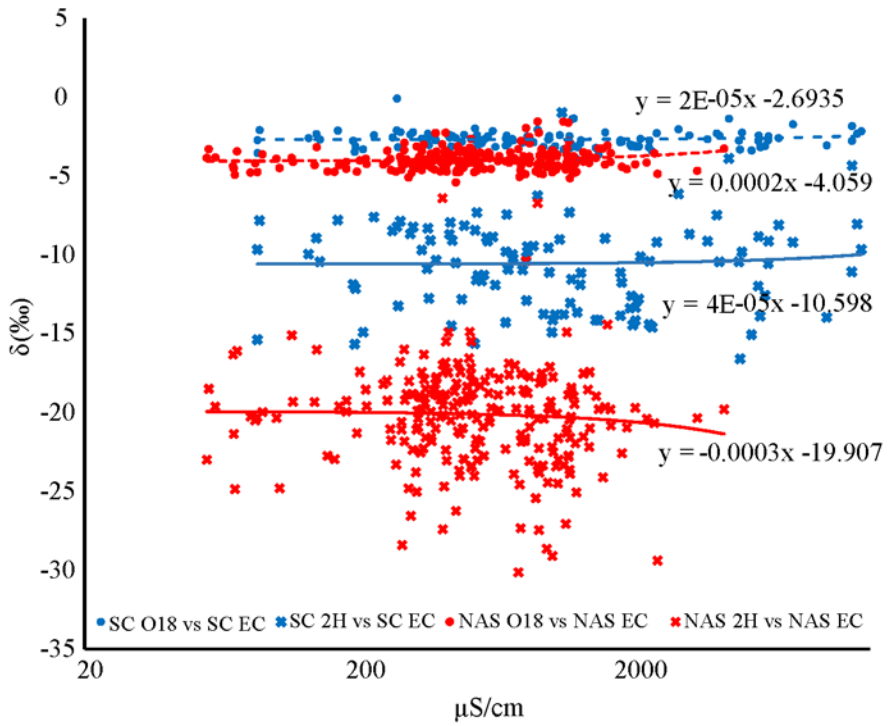

Figure 11: Relationship between stable isotopic composition content with electrical conductivity of SC and NAS samples respectively.